

Error-rejecting quantum computing with solid-state spins assisted by low-Q optical microcavities*

Tao Li and Fu-Guo Deng[†]

*Department of Physics, Applied Optics Beijing Area Major Laboratory,
Beijing normal University, Beijing 100875, China*

(Dated: June 17, 2018)

We present an efficient proposal for error-rejecting quantum computing with quantum dots (QD) embedded in single-sided optical microcavities based on the interface between the circularly polarized photon and QDs. An almost unity fidelity of the quantum entangling gate (EG) can be implemented with a detectable error that leads to a recycling EG procedure, which improves further the efficiency of our proposal along with the robustness to the errors involved in imperfect input-output processes. Meanwhile, we discuss the performance of our proposal for the EG on two solid-state spins with currently achieved experiment parameters, showing that it is feasible with current experimental technology. It provides a promising building block for solid-state quantum computing and quantum networks.

I. INTRODUCTION

Compared with the traditional computer, quantum computing [1] can factor an n -bit integer with the magical Shor algorithm [2], exponentially faster than the best-known classical algorithms. It can also run the famous quantum search algorithm, the Grover algorithm [3] or the optimal Long algorithm [4], for unsorted database search, which requires $O(\sqrt{N})$ operations only, rather than $O(N)$ operations involved in its classical counterpart. Both circuit-based quantum computing and the measurement-based one require quantum entangling gates. That is, the ability to entangle the quantum bits (qubits) is an essential building block in the construction of a quantum computer [1]. Since the early quantum entangling gate (EG) for single atoms was designed with the assistance of a high-Q optical cavity [5], more and more attention has been paid to the entangling operation between stationary qubits [5–13].

The previous EG between two stationary qubits is implemented by various methods that resort to different interactions, i.e., the coherent control of the direct qubit-qubit interaction, the indirect interaction mediated with high-Q optical cavities [5–10], or the controllable exchange interaction involved in the solid-state spin systems [11–13]. The typical absence of a heralding measurement in the EG resulting from the direct or indirect qubit-qubit interaction will lead to some ambiguous error, such as the one originating from the photon loss as a result of the cavity decay or the radiative deexcitation of the stationary dipole. These proposals could work successfully under the condition that the amount of noise involved in these EGs is less than a small threshold value [14]. It will be more physical-resource consuming and largely increase the complexity of the target quantum system when performing scalable quantum computing

with EGs of a higher error probability [15, 16]. However, with a layered quantum-computer architecture, the resources required for error correction will become manageable when the physical error rate is about an order of magnitude below the threshold value of the chosen code [16].

An alternative strategy exploits a measurement on the auxiliary photonic qubits that entangle with the corresponding stationary qubits to project the target stationary system into an entangled state, which constitutes a quantum EG of high fidelity. Meanwhile, its success is heralded by the detection of photons [17–25]. Its fidelity does not suffer from the photon loss noise, and it is relatively robust to the variation of the system parameters. Since these special schemes involve the optical Bell-state measurement (BSM) assisted by linear optical elements, they can succeed with the maximal efficiency of $1/2$ in the ideal situation [26, 27]. Besides the nondeterministic efficiency, the two photons for the BSM are required to be indistinguishable in all degrees of freedom except for the one used to encode the quantum information [28]. Therefore, if the polarization degree of freedom of photons is used to encode the photonic qubit, it will result in a smooth degradation in the performance of these EGs when the photonic spectral differences and the practical experimental control of the arrival time of the photons are considered.

It is well known that solid-state spin systems offer a promising candidate for the realization of quantum computing [29–31]. Its solid-state nature combined with nanofabrication techniques provide a relatively simple way to incorporate the spins into optical microcavities and allow for the generation of arrays of solid qubits [32–35]. One attractive type of solid-state spin system is the electron spin in a quantum dot (QD) [35–37]. Not only does it provide easy ways of optical initialization, single-qubit manipulation, and readout, but also it processes a long coherence time of the electron spin in QDs, which is typically around several microseconds when spin echo techniques are used [38–41]. Most existing quantum computing schemes based on single photons and single spins

*Published in Phys. Rev. A **94**, 062310 (2016)

[†]Corresponding author: fgdeng@bnu.edu.cn

in QDs are performed in a strong coupling regime as a result of cavity quantum electrodynamics (QED) [35, 42–45]. However, the strong coupling regime remains a challenge and some EG proposals for QDs in a low-Q cavity are proposed at the price of a decrease in the fidelity and the efficiency of the EG [46–50]. Meanwhile, the solid-state spins used in quantum computing are supposed to be homogeneous and the inhomogeneity of the spins will further decrease the feasibility of the proposed solid-state spin quantum computing [30].

In this article, we propose a robust proposal for the quantum EG between two QDs embedded in single-sided microcavities [42]. It is a practical proposal for performing efficient solid-state quantum computing that overcomes the existing limitations, since the fidelity of the EG for two QDs is always towards unity and the efficiency of the EG can, in principle, also approach unity. Compared with previous EGs for QDs based on cavity QED [43–48], the present scheme also has several other advantages. First, it does not require the strong-coupling limit and can work efficiently in low-Q cavities or even in the regime of resonance scattering [48] where the modified spontaneous emission parameter of QDs coupled resonantly to a microcavity is matched to that in the bulk dielectric. Second, the success of our EG is heralded with fidelity larger than 0.99, and it is signaled by the detection of a photon of orthogonal polarization as a result of cavity QED [51], where only one effective input-output process is involved in single-sided cavities, similar to the one in a nitrogen-vacancy center coupled to two-sided cavities [52]. This is the origin of our high efficiency rather than the maximal efficiency $1/8$ based on two-sided cavities. Third, the imperfect reflection of the cavity due to the deviation from the ideal conditions, i.e., the nonzero photonic bandwidth, the finite coupling rate between the QD and cavity mode, and the mismatch between the incident photon and the cavity mode, can only lead to photon loss or a click on either vertical detector rather than a decrease in the fidelity of the EG. Meanwhile, the QD subsystem will be collapsed into the original state when one of vertical detectors clicks, and we can input another probe photon to restart the EG directly without any re-preparation of the QDs, which makes our proposal more efficient than others. With our EGs, one can implement universal quantum computing, including both the one-way quantum computing and the circuit one [1].

II. ERROR-REJECTING ENTANGLING GATE FOR TWO QDS IN LOW-Q OPTICAL MICROCAVITIES

Let us consider a quantum system consisting of a singly charged self-assembled In(Ga)As QD embedded in a single-sided micropillar cavity [34, 42–44]. The quantization axis z is chosen along the growth direction of the QD and is also parallel to the light propagation direc-

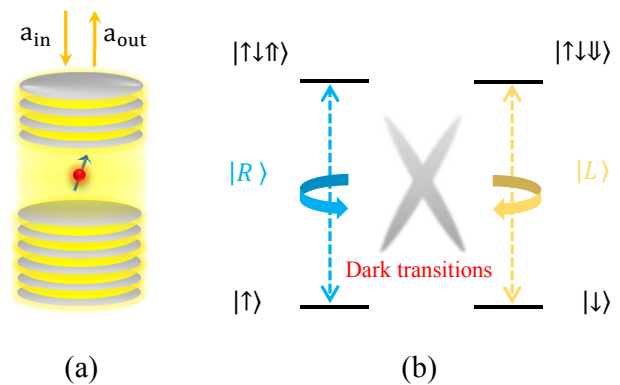


FIG. 1: The spin-dependent transitions for negatively charged exciton X^- . (a) A singly charged QD inside a single-sided optical micropillar cavity. (b) The relative energy levels and the optical transitions of a QD.

tion, shown in Fig. 1(a). The dipole transition associated with the negatively charged QD is strictly governed by Pauli’s exclusion principle [53], shown in Fig. 1(b). The single electron ground states have $J_z = \pm 1/2$, denoted $|\uparrow\rangle$ and $|\downarrow\rangle$, respectively, and the optical excited states are the trion states ($X^- = \{|\uparrow\downarrow\uparrow\rangle$ or $|\uparrow\downarrow\downarrow\rangle\}$) consisting of two antisymmetric electrons in the singlet state $1/\sqrt{2}(|\uparrow\downarrow\rangle - |\downarrow\uparrow\rangle)$ and one hole with $J_z = \pm 3/2$ ($|\uparrow\uparrow\rangle$ and $|\downarrow\downarrow\rangle$). The dipole-allowed transitions between the ground state and the trion state are $|\uparrow\rangle \leftrightarrow |\uparrow\downarrow\uparrow\rangle$ and $|\downarrow\rangle \leftrightarrow |\uparrow\downarrow\downarrow\rangle$, along with the absorption of a right-handed circularly polarized photon $|R\rangle$ and a left-handed one $|L\rangle$, respectively, while the crossing transitions are dipole forbidden [53].

When a circularly polarized probe photon is launched into the single-sided cavity, it will be reflected by the cavity with a spin-dependent reflection coefficient $r_j(\omega)$ [34, 42–44]. The dynamic process can be represented by Heisenberg equations for the cavity field operator \hat{a} and dipole operator $\hat{\sigma}_-$ in the interaction picture [54],

$$\begin{aligned} \frac{d\hat{a}}{dt} &= - \left[i(\omega_c - \omega) + \frac{\kappa}{2} + \frac{\kappa_s}{2} \right] \hat{a} - g\hat{\sigma}_- - \sqrt{\kappa}\hat{a}_{in} + \hat{R}, \\ \frac{d\hat{\sigma}_-}{dt} &= - \left[i(\omega_{X^-} - \omega) + \frac{\gamma}{2} \right] \hat{\sigma}_- - g\hat{\sigma}_z \hat{a} + \hat{N}, \end{aligned} \quad (1)$$

where ω_{X^-} , ω_c , and ω are the frequencies of the dipole transition, the cavity resonance, and the probe photon, respectively. \hat{R} and \hat{N} are noise operators which help to preserve the desired commutation relations. The parameter g is the coupling strength between X^- and the cavity mode. κ describes the coupling to the input and output ports, while κ_s and γ represent the cavity leakage rate and the trion X^- decay rate, respectively. In the weak excitation limit where the QD dominantly occupies the ground state, assisted by the standard cavity input-output theory $\hat{a}_{out} = \hat{a}_{in} + \sqrt{\kappa}\hat{a}$ [54], one can obtain the

spin-dependent reflection coefficient [42, 43, 55, 56]:

$$r_j(\omega) = 1 - \frac{\kappa \left[i(\omega_{X^-} - \omega) + \frac{\gamma}{2} \right]}{\left[i(\omega_{X^-} - \omega) + \frac{\gamma}{2} \right] \left[i(\omega_c - \omega) + \frac{\kappa}{2} + \frac{\kappa_s}{2} \right] + jg^2}. \quad (2)$$

Here the subscript j is used to discriminate the case that the polarized probe photon agrees with the trion transition ($j = 1$) and feels a QD-cavity coupled system and the case that the polarized photon decouples from the trion transition ($j = 0$) and feels an empty cavity.

Suppose the electron spin s of a QD is initialized to $|\psi_s\rangle = \alpha|\uparrow\rangle_s + \beta|\downarrow\rangle_s$, with $|\alpha|^2 + |\beta|^2 = 1$. When the input photon is in the polarized state $|\psi_p\rangle = \frac{1}{\sqrt{2}}(|R\rangle_p - |L\rangle_p)$, the photon reflected by the cavity directly due to the mismatching between the incident probe photonic field and the cavity mode, or reflected by the desired cavity-QD system, together with the QD, evolves into an unnormalized state

$$\begin{aligned} |\Phi\rangle_H &= \frac{\eta_{in}}{\sqrt{2}} \left[(r_1 \times \alpha|\uparrow\rangle_s + r_0 \times \beta|\downarrow\rangle_s) \otimes |R\rangle_p \right. \\ &\quad \left. - (r_0 \times \alpha|\uparrow\rangle_s + r_1 \times \beta|\downarrow\rangle_s) \otimes |L\rangle_p \right] \\ &\quad + \sqrt{1 - \eta_{in}^2} |\psi_s\rangle \otimes |\psi_p\rangle. \end{aligned} \quad (3)$$

Here η_{in} is the probability amplitude of the photon reflected by the desired cavity-QD system [57]. If one rewrites $|\Phi\rangle_H$ with the linear-polarization basis $\{|H\rangle \equiv \frac{1}{\sqrt{2}}(|R\rangle + |L\rangle), |V\rangle \equiv \frac{1}{\sqrt{2}}(|R\rangle - |L\rangle)\}$, one can get the system composed of the photon p and the electron spin s evolving into a partially entangled hybrid state,

$$\begin{aligned} |\Phi\rangle_{H_0} &= \left[\frac{\eta_{in}}{2} (r_1 + r_0) + \sqrt{1 - \eta_{in}^2} \right] (\alpha|\uparrow\rangle + \beta|\downarrow\rangle)_s \otimes |V\rangle_p \\ &\quad + \frac{\eta_{in}(r_1 - r_0)}{2} (\alpha|\uparrow\rangle - \beta|\downarrow\rangle)_s \otimes |H\rangle_p. \end{aligned} \quad (4)$$

Here the photon p is partially entangled with the electron spin s , and one can determine the state of the spin according to the outcome of the measurement on photon p . In detail, the detection of an $|H\rangle_p$ photon leads to a phase-flip operation on spin s . Alternatively, the detection of a $|V\rangle_p$ photon signals an error and results in an unchanged electron spin s , no matter where the error originates (the mismatch between the incident field and the cavity mode, the low-Q cavity, or the detuning). For simplicity, we can take $\eta_{in} \equiv 1$ below, since it will not affect the dominant performance of our EG protocol, and can only reduce the efficiency of our protocol by the amount of $1 - \eta_{in}^2$. Meanwhile, the output state of the combined hybrid system composed of the spin s and the probe photon p only depends on the combined coefficients $r_1 - r_0$ or $r_1 + r_0$ of the cavity-QD system, while it is independent of the particular parameters that affect the reflection coefficients r_j , shown in Eq. (2). Therefore, the output states of two individual inhomogeneous electron spins embedded in different optical microcavities along

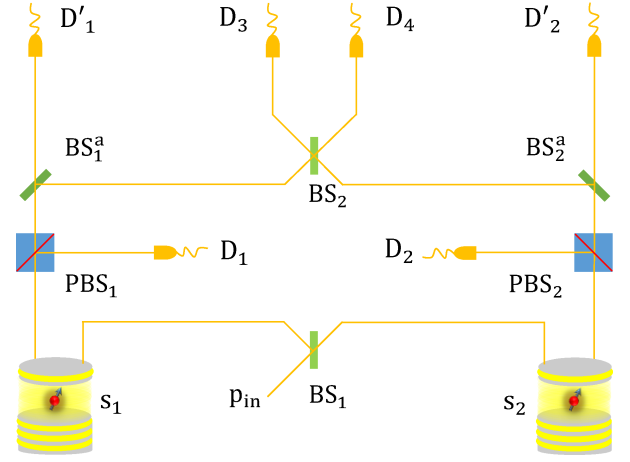


FIG. 2: The schematic setup of the EG. BS represents a 50 : 50 beam splitter. PBS is the polarizing beam splitter that transmits $|H\rangle$ photons and reflects $|V\rangle$ photons. BS_i^a denotes the beam splitter with adjustable reflection coefficient r_i^a , i.e., $r_1^a = r_2^a = 1$ is utilized for two identical cavity-QD systems; otherwise, $|r_1^a r_2^a| < 1$ that might lead to the click of single-photon detector D_i' and restart the recycling procedure before a phase-flip operation on spin s_i .

with their respective probe photons could be amended to be the same one by utilizing an adjustable beam splitter [51, 58]. The negative effect of the inhomogeneity of the solid-state spins could be eliminated formally, which leads to the same result as in homogeneous cavity-QD systems [34, 42–44].

With the faithful process described above, we can construct an error-rejecting EG, shown in Fig. 2, for two identical electron spins s_1 and s_2 (the reflection coefficients $r_i^a = 1$ of the adjustable beam splitter BS_i^a are adopted), which will collapse spins s_1 and s_2 into a state with a deterministic parity after the entangling process. Suppose the electron s_i ($i = 1, 2$) is initially in the state $|\Phi\rangle_{s_i} = \alpha_i|\uparrow\rangle_{s_i} + \beta_i|\downarrow\rangle_{s_i}$ with $|\alpha_i|^2 + |\beta_i|^2 = 1$. One probe photon p in state $|\Phi\rangle_p = \frac{1}{\sqrt{2}}(|R\rangle_p - |L\rangle_p)$ launched into the import of the EG passes through the beam splitter (BS_1), and it will be reflected by either the left cavity containing the electron spin s_1 or the right one containing s_2 . The unnormalized state of the hybrid system composed of the photon p and the electron spins s_1 and s_2 after being reflected by the cavities evolves into

$$\begin{aligned} |\Phi\rangle_{H_1} &= \frac{1}{\sqrt{2}} \left\{ (r_1 + r_0) (\alpha_1|\uparrow\rangle + \beta_1|\downarrow\rangle)_{s_1} (\alpha_2|\uparrow\rangle + \beta_2|\downarrow\rangle)_{s_2} \right. \\ &\quad \otimes (|V\rangle_{p_1} + |V\rangle_{p_2}) + (r_1 - r_0) [(\alpha_1|\uparrow\rangle - \beta_1|\downarrow\rangle)_{s_1} \\ &\quad \otimes (\alpha_2|\uparrow\rangle + \beta_2|\downarrow\rangle)_{s_2} |H\rangle_{p_1} + (\alpha_1|\uparrow\rangle + \beta_1|\downarrow\rangle)_{s_1} \\ &\quad \left. \otimes (\alpha_2|\uparrow\rangle - \beta_2|\downarrow\rangle)_{s_2} |H\rangle_{p_2} \right\}. \end{aligned} \quad (5)$$

Here the subscripts p_1 and p_2 denote photon components that occupy the left path and the right path, respectively. When the photon is in the horizontal polarized state $|H\rangle_{p_1}$

or $|H\rangle_{p_2}$, the two different spatial modes of photon p are combined on the BS₂. The interference of $|H\rangle_{p_1}$ and $|H\rangle_{p_2}$ modes will collapse the hybrid system into

$$|\Phi\rangle_{H_2} = \frac{1}{2}(r_1 - r_0)[(\alpha_1\alpha_2|\uparrow\rangle_{s_1}|\uparrow\rangle_{s_2} - \beta_1\beta_2|\downarrow\rangle_{s_1}|\downarrow\rangle_{s_2})|H\rangle_{p_3} + (\alpha_1\beta_2|\uparrow\rangle_{s_1}|\downarrow\rangle_{s_2} - \beta_1\alpha_2|\downarrow\rangle_{s_1}|\uparrow\rangle_{s_2})|H\rangle_{p_4}]. \quad (6)$$

Upon a click of the detector D_3 or D_4 , the EG is completed and the electron-spin system s_1s_2 is projected into a subspace with a deterministic parity, which is independent of the reflection coefficients r_j , since r_j only appears as a global coefficient in Eq. (6). In detail, when the photon detector D_3 clicks, the spins s_1s_2 collapse into the even-parity entangled state of the form

$$|\Phi\rangle_E = \alpha_1\alpha_2|\uparrow\rangle_{s_1}|\uparrow\rangle_{s_2} - \beta_1\beta_2|\downarrow\rangle_{s_1}|\downarrow\rangle_{s_2}. \quad (7)$$

When the photon detector D_4 clicks, the spins s_1s_2 are projected into the odd-parity entangled state of the following form

$$|\Phi\rangle_O = \alpha_1\beta_2|\uparrow\rangle_{s_1}|\downarrow\rangle_{s_2} - \beta_1\alpha_2|\downarrow\rangle_{s_1}|\uparrow\rangle_{s_2}. \quad (8)$$

Both states $|\Phi\rangle_E$ and $|\Phi\rangle_O$ keep the information of the initial state. Therefore, the coefficient α_i and β_j could be the state of other QD spins that are entangled with s_1 and s_2 , which makes the EG effective for constructing cluster states in the next section. The total probability that either D_3 or D_4 detects one photon of horizontal polarization is η_H :

$$\eta_H = \frac{|r_1 - r_0|^2}{4}. \quad (9)$$

Here η_H equals the efficiency of the EG without recycling procedure.

The first term on the right-hand side of Eq. (5) contains the vertical polarization component $|V\rangle_{p_1}$ ($|V\rangle_{p_2}$) and it will lead to a click on the photon detector D_1 (D_2). In this time, the state of the electron spins s_1s_2 is projected into $|\Phi\rangle_{s_1} \otimes |\Phi\rangle_{s_2}$, exactly identical to the original one without any interaction between the spins and the photon p , which takes place with probability η_V :

$$\eta_V = \frac{|r_1 + r_0|^2}{4}. \quad (10)$$

Here η_V equals the heralded error efficiency of the EG, and the electron spins s_1s_2 , in this case, could be directly used in the recycling EG procedure.

In a word, one can obtain two kinds of useful results with our EG setup. When only one probe photon is exploited, the probabilities of heralded success or failure of the EG are η_H or η_V , respectively. When the heralded error of EG takes place, a $|V\rangle$ polarized photon is detected and the state of the spin subsystem has not been changed. One can input another probe photon p' in state $|\Phi\rangle_{p'} = \frac{1}{\sqrt{2}}(|R\rangle - |L\rangle)_{p'}$ to repeat the EG process until a horizontal photon $|H\rangle$ is detected by D_3 or

D_4 . This procedure will project the spin system s_1s_2 into an even-parity subspace or an odd-parity one eventually. By taking the recycling procedure into account, the total success probability η_S of our error-rejecting EG is

$$\eta_S = \frac{|r_1 - r_0|^2}{4 - |r_1 + r_0|^2}, \quad (11)$$

which is state independent, resulting in a more efficient quantum computing [1]. Note that each recycling procedure is conditioned on a click of either vertical detector D_1 or D_2 , and it should be stopped when photon loss takes place. Subsequently, one has to reinitialize the spins before performing a new EG operation on the spins.

III. CLUSTER STATE GENERATION WITH OUR EG FOR MEASUREMENT-BASED ONE-WAY QUANTUM COMPUTING

Our error-rejecting EG can be used directly to implement the one-way quantum computing [30, 59, 60] based on QDs embedded in optical cavities. In the following, we demonstrate that our EG can be used to construct the two-dimensional (2D) QD cluster state [30, 61, 62], which constitutes the base of one-way quantum computing on solid-state spins.

Suppose there are $j + 1$ QD electron spins $\{s_1, s_2, \dots, s_j\}$ and s_{j+1} , and s_{j+1} is initialized to be the state $\frac{1}{\sqrt{2}}(|\uparrow\rangle_{j+1} - |\downarrow\rangle_{j+1})$ and the first j spins are initially in the one-dimensional (1D) cluster state of the form

$$|\psi_j\rangle = (|\uparrow\rangle_1 + |\downarrow\rangle_1 \hat{Z}_2)(|\uparrow\rangle_2 + |\downarrow\rangle_2 \hat{Z}_3) \cdots \otimes (|\uparrow\rangle_{j-1} + |\downarrow\rangle_{j-1} \hat{Z}_j)(|\uparrow\rangle_j + |\downarrow\rangle_j), \quad (12)$$

with the phase flip operator $\hat{Z}_i = |\uparrow\rangle_i \langle \uparrow| - |\downarrow\rangle_i \langle \downarrow|$. To increase the length of the 1D cluster state, an error-rejecting EG for spins s_j and s_{j+1} is applied. When the EG fails, the state of spin s_j is ambiguous and a state measurement on s_j with basis $\{|\uparrow\rangle, |\downarrow\rangle\}$ will collapse the remaining spins into a 1D cluster state of $j - 1$ qubits, with or without a \hat{Z}_{j-1} feedback operation. When the EG succeeds in the case that is heralded by the click of photon detector D_3 , the $j + 1$ spins will be projected into

$$|\psi'_{j+1}\rangle = (|\uparrow\rangle_1 + |\downarrow\rangle_1 \hat{Z}_2)(|\uparrow\rangle_2 + |\downarrow\rangle_2 \hat{Z}_3) \cdots (|\uparrow\rangle_{j-1} + |\downarrow\rangle_{j-1} \hat{Z}_j)(|\uparrow\rangle_j |\uparrow\rangle_{j+1} + |\downarrow\rangle_j |\downarrow\rangle_{j+1}), \quad (13)$$

which could be transformed into the 1D cluster state similar to that in Eq. (12) of length $j + 1$ by a Hadamard operation \hat{H}_j [\hat{H} completes the following transformation: $|\uparrow\rangle \rightarrow \frac{1}{\sqrt{2}}(|\uparrow\rangle + |\downarrow\rangle)$ and $|\downarrow\rangle \rightarrow \frac{1}{\sqrt{2}}(|\uparrow\rangle - |\downarrow\rangle)$] performed on spin j . If the success of the EG for s_j and s_{j+1} is signaled by the click of D_4 , a local operation $\hat{H}_{j+1} \hat{X}_{j+1}$ (here the spin-flip operator $\hat{X} = |\uparrow\rangle \langle \downarrow| + |\downarrow\rangle \langle \uparrow|$) on spin

s_{j+1} could also evolve the $j + 1$ spins into the desired 1D cluster state.

This procedure of cluster growth discussed above could be used to generate a larger cluster, since the efficiency of our error-rejecting EG $\eta_s > 0.5$ and can, in principle, approach unity. To speed up the cluster generation process, some shorter clusters could be prepared in parallel and then be connected together to generate the longer one [27, 63, 64]. In the following, we introduce an efficient cluster-connecting proposal. Suppose the two 1D clusters M and N available are, respectively, of lengths m and n ,

$$|\psi_m\rangle = (|\uparrow_M\rangle_1 + |\downarrow_M\rangle_1 \hat{Z}_{M_2}) \cdots (|\uparrow_M\rangle_{m-1} + |\downarrow_M\rangle_{m-1} \hat{Z}_{M_m})(|\uparrow_M\rangle_m + |\downarrow_M\rangle_m), \quad (14)$$

$$|\psi_n\rangle = (|\uparrow_N\rangle_1 + |\downarrow_N\rangle_1 \hat{Z}_{N_2}) \cdots (|\uparrow_N\rangle_{n-1} + |\downarrow_N\rangle_{n-1} \hat{Z}_{N_n})(|\uparrow_N\rangle_n + |\downarrow_N\rangle_n). \quad (15)$$

Before performing EG on M_m and N_1 , a phase-flip operation \hat{Z}_{M_m} is applied on spin M_m . The success of the EG heralded by the click of photon detector D_3 will project the entire spin system into

$$|\psi_m^n\rangle = (|\uparrow_M\rangle_1 + |\downarrow_M\rangle_1 \hat{Z}_{M_2}) \cdots (|\uparrow_M\rangle_{m-1} + |\downarrow_M\rangle_{m-1} \hat{Z}_{M_m})(|\uparrow_M\rangle_m |\uparrow_N\rangle_1 + |\downarrow_M\rangle_m |\downarrow_N\rangle_1 \hat{Z}_{N_2}) \cdots (|\uparrow_N\rangle_{n-1} + |\downarrow_N\rangle_{n-1} \hat{Z}_{N_n})(|\uparrow_N\rangle_n + |\downarrow_N\rangle_n). \quad (16)$$

An additional Hadamard operation \hat{H} on M_m will evolve the spin system into a 1D cluster $|\psi_{m+n}\rangle$ of $m+n$ qubits. As for the case that the success of the EG is signaled by a click of detector D_4 , a local single-qubit operation $\hat{H}\hat{X}$ on M_m can also evolve the $m+n$ spins into the 1D cluster $|\psi_{m+n}\rangle$.

The cluster-connecting procedure based on parity measurement above is similar to that used in linear optical quantum computing [65], whereas both the outcome of the EG operation and the feedback operations after the EG are quite different. It generates a 1D cluster of $m+n$ qubit, rather than $m+n-1$ in linear optical quantum computing [65] or in previous schemes for solid-state spins [27] in which the outcomes of the EG can only lead to an odd parity and the cluster connecting procedure is completed by a spin measurement later. One can also perform a cross-linking between linear chains to construct a 2D cluster similar to the previous schemes [27, 63–65], which means our EG can be used to complete universal one-way quantum computing efficiently.

IV. PERFORMANCE OF OUR ERROR-REJECTING EG WITH CURRENT EXPERIMENTAL PARAMETERS

The total success probability η_s together with η_H and η_V of our EG are shown in Fig. 3 as a function of the side leakage κ/κ_s with the cooperativity $C \equiv g^2/\gamma\kappa_T$,

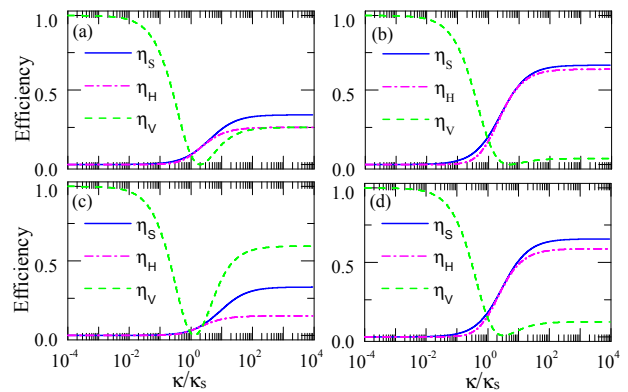


FIG. 3: The efficiency of the EG vs different parameters with $\omega_{X^-}/\omega_c = 1$ and $\gamma/\kappa = 0.1$: (a) $(\omega_c - \omega)/\kappa = 0$, $C = 1/4$; (b) $(\omega_c - \omega)/\kappa = 0$, $C = 1$; (c) $(\omega_c - \omega)/\kappa = \gamma/\kappa$, $C = 1/4$; and (d) $(\omega_c - \omega)/\kappa = \gamma/\kappa$, $C = 1$.

$\kappa_T \equiv \kappa_s + \kappa$, and $\gamma/\kappa = 0.1$ [66]. We tune the transition frequency ω_{X^-} of the QD to be resonant to that of the cavity, $\omega_{X^-}/\omega_c = 1$ [67]. When the probe photon is also resonant to cavity [see Figs. 3 (a) and (b)], $\eta_S^r = 0.255$ and $\eta_S^p = 0.559$ can be achieved in the regime of resonance scattering with $C = 1/4$ and the Purcell regime with $C = 1$, respectively, for $\kappa/\kappa_s = 13$ [48, 68]. When the probe photon detunes from the trion transition by $(\omega_c - \omega)/\kappa = \gamma/\kappa$, shown in Figs. 3 (c) and (d), $\eta_S^r = 0.194$ and $\eta_S^p = 0.538$ can be achieved for the same remaining parameters, and the contribution from the recycling procedure η_V increases. Furthermore, the EG could enjoy a higher efficiency with a lower side leakage and a higher cooperativity C , which can be achieved by utilizing adiabatic cavities with smaller pillar diameters [66, 68]. In other words, the near-unity efficiency of the error-rejecting EG can be achieved when the deep Purcell regime with low side leakage is available, and we can easily attribute this improvement of the efficiency to the enhancement of the photon into the cavity mode.

In the above discussion, we can get an efficient error-rejecting EG for QDs with the perfect spin qubit and the monochromatic (δ -function-like) single photon wavepacket. In fact, every single photon pulse is of finite linewidth, i.e., a polarized photon of pulse shape in Gaussian function $f(\omega) = \exp(-\omega^2/\Delta^2)/(\sqrt{\pi}\Delta)$ with bandwidth Δ . This finite-linewidth character usually introduces some additional infidelity in the previous EG protocols [42–50], while it has little harmful effect on the fidelity of our EG. When one constitutes our EG with a polarized single-photon pulse p of Gaussian shape, $|\psi_p\rangle = \frac{1}{\sqrt{2}} \int d\omega f(\omega) [\hat{a}_R^\dagger(\omega) - \hat{a}_L^\dagger(\omega)] |0\rangle$, where $\hat{a}_k^\dagger(\omega)$ is the creation operator of a k -polarized photon with frequency ω , the state of the hybrid system composed of the photon p and electron spins s_1 and s_2 just before photon

detection process, shown in Eq. (6), will be modified to

$$|\Phi\rangle_{H_2} = \frac{1}{2} \int d\omega [r_1(\omega) - r_0(\omega)] f(\omega) \left\{ (\alpha_1 \alpha_2 |\uparrow\rangle_{s_1} |\uparrow\rangle_{s_2} - \beta_1 \beta_2 |\downarrow\rangle_{s_1} |\downarrow\rangle_{s_2}) \otimes \hat{a}_H^\dagger(\omega) |0\rangle_{p_3} + (\alpha_1 \beta_2 |\uparrow\rangle_{s_1} |\downarrow\rangle_{s_2} - \beta_1 \alpha_2 |\downarrow\rangle_{s_1} |\uparrow\rangle_{s_2}) \otimes \hat{a}_H^\dagger(\omega) |0\rangle_{p_4} \right\}, \quad (17)$$

where $\hat{a}_H^\dagger(\omega) = \frac{1}{\sqrt{2}}[\hat{a}_R^\dagger(\omega) + \hat{a}_L^\dagger(\omega)]$. Upon the click of photon detector D_3 or D_4 , one can still complete the EG by projecting spins s_1 and s_2 into a subspace of determined parity, as one does with a monochromatic photon wave packet. One can find that the fidelity of our EG is independent of the finite linewidth of the photon pulse, since the frequency-dependent reflection coefficients $r_j(\omega)$ appear only in the global coefficient.

In fact, the effects of dephasing and decay of electron spins will affect the performance of the EG. The time needed for the coherent control of single electron spin in QDs is on the scale of picoseconds [38, 39] and the cavity photon time is tens of picoseconds when the cavity Q -factor is about $1 \times 10^4 - 1 \times 10^5$ [66]. Therefore, it is the spontaneous emission lifetime of a QD, which is about 1 ns, that sets the upper limit for the fidelity of the EG. Meanwhile, the electron spin coherence time of 10 ns has been achieved at zero magnetic field [69], and it could be extended to several microseconds if the all-optical spin echo technique is exploited [40, 41]. The ratio of the decoherence time of electron spins to the operation time needed to complete the EG can exceed 1×10^3 , and thus the fidelity of the EG proposal will be larger than 0.99 when taking into account the dephasing process of the electron spin, which suggests the strong promise of electron spin in QDs for scalable quantum computing.

V. DISCUSSION AND SUMMARY

Our scheme of error-rejecting EG can work efficiently with almost unity fidelity in the strong coupling regime, $g > \kappa_T, \gamma$, the Purcell regime, $C > 1/4$, or even the resonantly scattering regime, $C = 1/4$. It is robust to the imperfections involved in the practical input-output process, i.e., the nonzero bandwidth, QD or cavity decay, and the finite coupling g/κ , since the fidelity of our EG is independent of the reflective coefficients $r_j(\omega)$ and thus independent of the cooperativity C , which is far different from other schemes that depends on C [43–48]. The original low fidelity or error items originating from the practical input-output process are converted into a relatively lower efficiency in our EG. Fortunately, the low fidelity or error items trigger the single-photon detector D_1 or D_2 , which can be used to improve the efficiency of the EG by introducing the recycling procedure. In fact, our recycling procedure can contribute little when perfect circular birefringence ($C \gg 1$ and $\omega_{X^-} = \omega_c = \omega$) is available, since the efficiency η_H of the EG without recycling procedure approaches unity in this situation. Although

our proposal is detailed with the QD-cavity system, it could also be implemented with solid-state spin coupled to a photonic crystal waveguide [70].

The previous EG performed in a resonantly scattering regime, $C = 1/4$ and $\omega_{X^-} = \omega_c = \omega$ could also be completed with high fidelity, since a reflectivity $r_1 = 0$ in the resonantly scattering regime could be automatically eliminated, and only the photon that decouples the electron spin could be reflected. Therefore, one can entangle two spins by subsequently probing the two spin-cavity systems with a linear polarized photon or entangle two linear polarized photons by subsequently importing them into a spin-cavity system, where the even-parity subspace of the spin system or the photon system could be easily picked out, since the odd-parity case will inevitably be signaled by photon loss [48], and the corresponding efficiency of the EG is 0.25. It is quite different from our EG where the linear polarized photon, after being reflected by the QD-cavity system, in the ideal case $C \gg 1$ and $\omega_{X^-} = \omega_c = \omega$, is supposed to change its polarization into the orthogonal polarization and exert a phase-flip operation on the spin. The interference of the photon after being reflected by two cavities in superposition can project the two spins into either even-parity subspace or odd-parity subspace in a heralded way.

The error-rejecting EG only involves one effective input-output process, which makes our scheme more efficient than others since the practical input-output coupling $\eta_{in} < 1$ [57]. In this situation, the probe photon can be reflected directly by the cavity, and it is harmful and will reduce the fidelity of the entangling process in the other schemes [21, 22, 43–48]. However, it can only lead to a decrease of the efficiency of our EG, since the state of the photon reflected directly by the microcavity together with that of the spins will be kept unchanged. In other words, the photon reflected directly by the microcavity is still in $|V\rangle$ polarization and it will trigger the single-photon detector D_1 or D_2 , which signals the restarting of the EG. This makes the EG different from the one based on a double-sided cavity where the photon is encoded in its Fock state [52]. The photon loss during the EG process owing to the inefficiency of the single-photon detector or cavity absorption will decrease the efficiency of the EG, but it does not affect the fidelity of our EG since both the success of the EG and the restarting of the EG are signaled by a click of single photon detectors.

In conclusion, we have proposed an efficient error-rejecting EG proposal for two electron spins of QDs embedded in low- Q optical microcavities. With our error-rejecting EGs, a cluster-state connection scheme could be completed efficiently. Under the practical experimental condition, the EG could be performed well with almost unity fidelity and an efficiency of $\eta_s > 0.53$ for $C = 1$. We believe the EG could provide a promising building block for solid-state scalable quantum computing and quantum networks in the future.

ACKNOWLEDGMENTS

This work is supported by the National Natural Science Foundation of China under Grants No. 11474026

and No. 11674033, and the Fundamental Research Funds for the Central Universities under Grant No. 2015KJJC01.

-
- [1] M. A. Nielsen and I. L. Chuang *Quantum Computation and Quantum Information* (Cambridge University Press, Cambridge, UK, 2000).
- [2] P. W. Shor, *SIAM J. Sci. Statist. Comput.* **26**, 1484 (1997).
- [3] L. K. Grover, *Phys. Rev. Lett.* **79**, 325 (1997).
- [4] G. L. Long, *Phys. Rev. A* **64**, 022307 (2001).
- [5] J. I. Cirac and P. Zoller, *Phys. Rev. A* **50**, R2799 (1994).
- [6] J. I. Cirac, P. Zoller, H. J. Kimble, and H. Mabuchi, *Phys. Rev. Lett.* **78**, 3221 (1997).
- [7] M. D. Lukin and P. R. Hemmer, *Phys. Rev. Lett.* **84**, 2818 (2000).
- [8] S. B. Zheng and G. C. Guo, *Phys. Rev. Lett.* **85**, 2392 (2000).
- [9] E. Hagle, X. Maître, G. Nogues, C. Wunderlich, M. Brune, J. M. Raimond, and S. Haroche, *Phys. Rev. Lett.* **79**, 1 (1997).
- [10] J. Borregaard, P. Kómár, E. M. Kessler, A. S. Sørensen, and M. D. Lukin, *Phys. Rev. Lett.* **114**, 110502 (2015).
- [11] C. Piermarocchi, P. Chen, L. J. Sham, and D. G. Steel, *Phys. Rev. Lett.* **89**, 167402 (2002).
- [12] G. F. Quinteiro, J. Fernández-Rossier, and C. Piermarocchi, *Phys. Rev. Lett.* **97**, 097401 (2006).
- [13] R. B. Liu, W. Yao, and L. J. Sham, *Adv. Phys.* **59**, 703 (2010).
- [14] A. M. Steane, *Phys. Rev. A* **68**, 042322 (2003).
- [15] N. C. Jones, R. Van Meter, A. G. Fowler, P. L. McMahon, J. Kim, T. D. Ladd, and Y. Yamamoto, *Phys. Rev. X* **2**, 031007 (2012).
- [16] E. Knill, *Nature* **434**, 39 (2005).
- [17] L. M. Duan, M. Lukin, J. I. Cirac, and P. Zoller, *Nature* **414**, 413 (2001).
- [18] X. L. Feng, Z. M. Zhang, X. D. Li, S. Q. Gong, and Z. Z. Xu, *Phys. Rev. Lett.* **90**, 217902 (2003).
- [19] D. E. Browne, M. B. Plenio, and S. F. Huelga, *Phys. Rev. Lett.* **91**, 067901 (2003).
- [20] C. Simon and W. T. M. Irvine, *Phys. Rev. Lett.* **91**, 110405 (2003).
- [21] A. S. Sørensen and K. Mølmer, *Phys. Rev. Lett.* **90**, 127903 (2003).
- [22] A. S. Sørensen and K. Mølmer, *Phys. Rev. Lett.* **91**, 097905 (2003).
- [23] L. Childress, J. M. Taylor, A. S. Sørensen, and M. D. Lukin, *Phys. Rev. A* **72**, 052330 (2005).
- [24] L. M. Duan and C. Monroe, *Rev. Mod. Phys.* **82**, 1209 (2010).
- [25] P. Maunz, S. Olmschenk, D. Hayes, D. N. Matsukevich, L. M. Duan, and C. Monroe, *Phys. Rev. Lett.* **102**, 250502 (2009).
- [26] J. W. Pan, C. Simon, Č. Brukner, and A. Zeilinger, *Nature* **410**, 1067 (2001).
- [27] S. D. Barrett and P. Kok, *Phys. Rev. A* **71**, 060310 (2005).
- [28] N. Kalb, A. Reiserer, S. Ritter, and G. Rempe, *Phys. Rev. Lett.* **114**, 220501 (2015).
- [29] I. Buluta, S. Ashhab, and F. Nori, *Rep. Prog. Phys.* **74**, 104401 (2009).
- [30] S. C. Benjamin, B. W. Lovett, and J. M. Smith, *Laser Photon. Rev.* **3**, 556 (2009).
- [31] T. D. Ladd, F. Jelezko, R. Laflamme, Y. Nakamura, C. Monroe, and J. L. O'Brien, *Nature* **464**, 45 (2010).
- [32] D. Englund, B. Shields, K. Rivoire, F. Hatami, J. Vučković, H. Park, and M. D. Lukin, *Nano Lett.* **10**, 3922 (2010).
- [33] J. Zhang and D. Suter, *Phys. Rev. Lett.* **115**, 110502 (2015).
- [34] A. B. Young, R. Oulton, C. Y. Hu, A. C. T. Thijssen, C. Schneider, S. Reitzenstein, M. Kamp, S. Höfling, L. Worschech, A. Forchel, and J. G. Rarity, *Phys. Rev. A* **84**, 011803 (2011).
- [35] P. Lodahl, S. Mahmoodian, and S. Stobbe, *Rev. Mod. Phys.* **87**, 347 (2015).
- [36] D. Loss, and D. P. DiVincenzo, *Phys. Rev. A* **57**, 120 (1998).
- [37] A. Imamoglu, D. D. Awschalom, G. Burkard, D. P. DiVincenzo, D. Loss, M. Sherwin, and A. Small, *Phys. Rev. Lett.* **83**, 4204 (1999).
- [38] K. De Greve, D. Press, P. L. McMahon, and Y. Yamamoto, *Rep. Prog. Phys.* **76**, 092501 (2013).
- [39] J. Berezovsky, M. H. Mikkelsen, N. G. Stoltz, L. A. Col-dren, and D. D. Awschalom, *Science* **320**, 349 (2008).
- [40] D. Press, K. De Greve, P. L. McMahon, T. D. Ladd, B. Friess, C. Schneider, M. Kamp, S. Höfling, A. Forchel, and Y. Yamamoto, *Nat. Photon.* **4**, 367 (2010).
- [41] K. De Greve, P. L. McMahon, D. Press, T. D. Ladd, D. Bisping, C. Schneider, M. Kamp, L. Worschech, S. Höfling, A. Forchel, and Y. Yamamoto, *Nat. Phys.* **7**, 872 (2011).
- [42] C. Y. Hu, W. J. Munro, and J. G. Rarity, *Phys. Rev. B* **78**, 125318 (2008).
- [43] C. Y. Hu, A. Young, J. L. O'Brien, W. J. Munro, and J. G. Rarity, *Phys. Rev. B* **78**, 085307 (2008).
- [44] H. R. Wei and F. G. Deng, *Opt. Express* **22**, 593 (2014).
- [45] H. R. Wei and F. G. Deng, *Sci. Rep.* **4**, 7551 (2014).
- [46] K. Koshino and Y. Matsuzaki, *Phys. Rev. A* **86**, 020305 (2012).
- [47] E. Waks and J. Vučković, *Phys. Rev. Lett.* **96**, 153601 (2006).
- [48] A. B. Young, C. Y. Hu, and J. G. Rarity, *Phys. Rev. A* **87**, 012332 (2013).
- [49] A. Auffèves-Garnier, C. Simon, J. M. Gérard, and J. P. Poizat, *Phys. Rev. A* **75**, 053823 (2007).
- [50] C. Bonato, F. Haupt, S. S. R. Oemrawsingh, J. Gudat, D. Ding, M. P. van Exter, and D. Bouwmeester, *Phys. Rev. Lett.* **104**, 160503 (2010).
- [51] Y. Li, L. Aolita, D. E. Chang, and L. C. Kwek, *Phys. Rev. Lett.* **109**, 160504 (2012).
- [52] K. Nemoto, M. Trupke, S. J. Devitt, A. M. Stephens, B. Scharfenberger, K. Buczak, T. Nöbauer, M. S. Everitt, J. Schmiedmayer, and W. J. Munro, *Phys. Rev. X* **4**,

- 031022 (2014).
- [53] R. J. Warburton, *Nat. Mater.* **12**, 483 (2013).
- [54] D. F. Walls and G. J. Milburn, *Quantum Optics* (Springer, New York, 2008).
- [55] E. Waks and J. Vuckovic, *Phys. Rev. A* **73**, 041803 (2006).
- [56] J. H. An, M. Feng, and C. H. Oh, *Phys. Rev. A* **79**, 032303 (2009).
- [57] V. Loo, L. Lanco, A. Lemaître, I. Sagnes, O. Krebs, P. Voisin, and P. Senellart, *Appl. Phys. Lett.* **97**, 241110 (2010).
- [58] T. Li, G. J. Yang, and F. G. Deng, *Opt. Express.* **22**, 23897 (2014).
- [59] H. J. Briegel and R. Raussendorf, *Phys. Rev. Lett.* **86**, 910 (2001).
- [60] R. Raussendorf and H. J. Briegel, *Phys. Rev. Lett.* **86**, 5188–5191 (2001).
- [61] Y. S. Weinstein, C. S. Hellberg, and J. Levy, *Phys. Rev. A* **72**, 020304 (2005).
- [62] Z. R. Lin, G. P. Guo, T. Tu, F. Y. Zhu, and G. C. Guo, *Phys. Rev. Lett.* **101**, 230501 (2008).
- [63] L. M. Duan and R. Raussendorf, *Phys. Rev. Lett.* **95**, 080503 (2005).
- [64] L. M. Duan, M. J. Madsen, D. L. Moehring, P. Maunz, R. N. Kohn, and C. Monroe, *Phys. Rev. A* **73**, 062324 (2006).
- [65] D. E. Browne and T. Rudolph, *Phys. Rev. Lett.* **95**, 010501 (2005).
- [66] J. P. Reithmaier, G. Sek, A. Löffler, C. Hofmann, S. Kuhn, S. Reitzenstein, L. V. Keldysh, V. D. Kulakovskii, T. L. Reinecke, and A. Forchel, *Nature* **432**, 197 (2004).
- [67] J. Gudat, C. Bonato, E. van Nieuwenburg, S. Thon, H. Kim, P. M. Petroff, M. P. van Exter, and D. Bouwmeester, *Appl. Phys. Lett.* **98**, 121111 (2011).
- [68] M. Lermer, N. Gregersen, F. Dunzer, S. Reitzenstein, S. Höfling, J. Mørk, L. Worschech, M. Kamp, and A. Forchel, *Phys. Rev. Lett.* **108**, 057402 (2012).
- [69] M. H. Mikkelsen, J. Berezovsky, N. G. Stoltz, L. A. Coldren, and D. D. Awschalom, *Nat. Phys.* **3**, 770 (2007).
- [70] A. B. Young, A. C. T. Thijssen, D. M. Beggs, P. Androvitsaneas, L. Kuipers, J. G. Rarity, S. Hughes, and R. Oulton, *Phys. Rev. Lett.* **115**, 153901 (2015).